Print ISSN: 2321-6379
Online ISSN: 2321-595X
DOI: 10.17354/ijssl/2017/72

Original Article

Studying the Performance of Short Shear-Walls Considering Rocking Motion Effect

Mohammad Ghanizadeh[1], Masood Farzam[2], Ebrahim Ghanizadeh[3]

[1]MSc. in Structural Engineering, Tabriz University,Tabriz ,Iran, [2]Assistant Professor, Department of Structural Engineering, Tabriz University, Tabriz ,Iran, [3]MSc in Civil Engineering, Geotechnical Trends, Tabriz University, Tabriz ,Iran

Abstract

In wall-frame structures because of the large lateral stiffness of shear walls, the magnitude of the base shear force and overturning moment are high which cause to great uplift forces at the foundation. Tension piles commonly are needed to resist these forces that in turn increase the cost and time of the erection. Utilizing shallow foundations in low rise structures, it is possible to take into account the rocking behavior of foundation in addition to cutting the foundation cost. In this paper at first lateral behavior of a shallow flanged shear wall which have been experimentally tested by Nuclear Power Engineering Corporation of Japan (NUPEC) are studied numerically using nonlinear finite element software ATENA to recognize the impact of the concrete and steel models on its behavior. The software in addition to modeling the plastic behavior of concrete in compression, take to account the nonlinear behavior in tension based on fracture mechanics parameters. Moreover the bond- sliding models can be applied to all rebar's which has significant effect on the total behavior of adopted system. The CEB-FIP bond- sliding model results to better results in the studied wall. Furthermore, the rotated crack or stable crack models are studied. In rotated crack model it is possible to define a limit in the softening branch of the tension behavior of concert, which after that the inclination of the opened crack will be stable. Analyses show that for the shallow walls, the total stable crack model show better agreement with the experimentally observed cracks as well as the load-deflection curve. The brick elements with 8 node are used for meshing the wall. Only one half of the wall is modelled because of the symmetry in the geometry and the loading regime. The results show good agreement with test results. Afterward, the proposed wall geometry for strengthening of low rise masonry structures by International Institute of Earthquake Engineering and Seismology (IIEES) are studied numerically to understand the affecting parameters on its overall behavior. The length of foundation is increased from a practical minimum limit to extremely large length to study the effect of the rocking motion on the lateral load loading and the failure mode of the wall. It is shown that with increasing the length of foundation the lateral load loading capacity of shear walls showing rocking behavior is increased while the ductility is reduced. Considering this matter that in masonry structures, the length of wall is determined based on the architectural limitations, and it can be shown that the total lateral strength of wall need not to be mobilized. Consequently, counting on a lesser strength than the lateral failure load of wall, one can motivate the rocking behavior of the wall-substructure to increase the ductility of the wall which in turn increases the ductility of the structure. The length of foundation can be adopted based on the required lateral strength of wall and desired ductility level. It is shown that level of gravity loads can affect these mentioned parameters. Furthermore the different arrangement of reinforcement bars, specially using diagonally located bars can improve the ductility.

Key words: Short shear wall, Rocking motion, Stiffness, Shear strength

INTRODUCTION

Based on the conducted studies in retrofitting structures using shear wall, about one-third of retrofitting projects cost, including implementation of the foundation and candles. To reduce this amount the without candle shear wall is used through which the under seismic wall move in the rocking form. In the case of retrofitting the short-order buildings with shear walls, if the rocking motion is considered in designing the shear, the time and cost of the project can be reduced without the manipulation of the interiors in the same time with creating the resistance and good formability. The soil-foundation system result in energy loss during the rocking motion especially for shear wall system; while in elastic designing for the shear wall elements, less energy is lost. In order to use this energy

Access this article online

IJSS
www.ijss-sn.com

Month of Submission : 06-2017
Month of Peer Review : 06-2017
Month of Acceptance : 07-2017
Month of Publishing : 07-2017

Corresponding Author: Mohammad Ghanizadeh, MSc. in Structural Engineering. E-mail: ghanizadeh.md@gmail.com

loss under the foundations, the soil-foundation system is designed in a form as a mechanism for optimizing the structure performance so that the energy loss be maximum and reliable as well as the resulted permanent deformations under the foundation from its rocking motion be in the allowable range.

The estimation of the surface displacement foundations is fundamental problem in geotechnical engineering while they are under the vertical and shear combined loading and bending moment as well as under the static combined loadings even under conditions that the yield limit is reached. The dynamics interaction of soil and structural, materials (soil yield), geotechnical nonlinear properties (the foundation uplifting) and the nonlinear behavior associated with the load-displacement cyclic for foundation, leading to the challenges in relation to the analysis of the contact surface compatibility model of the soil-foundation during seismic loading.

A shear wall which is preserved by the shallow foundation system is a conventional resistant structural system against the seismic powers which its designations and performance need to be investigated and studied. Rocking motion is considered in different regulations such as FEMA 274 and FEMA 440. (1)(2). One of the main differences has been applied in the traditional seismic process at the NEHRP guideline of FEMA regulation in 1997(1), is as follow; the shallow foundation are let to use final capacity and rocking motion to reduce simple formation. But, in practice, the cases such as uncertainty in soil features, the lack of practical and reliable modeling techniques for the foundation and the under foundation permanent subsidence resulted from its rocking motion are considered as the obstacles for using soil construct-foundation non-liner interaction as a mechanism to reduce the damages of the system. Lots of researchers such as Georgiadis *et al.* (1985), Butterfield *et al.* (1988), Gottardi *et al.* (1993), Butterfield *et al.* (1995) and Gottardi *et al.* (1999) conducted theoretical and experimental researches on the rocking motion. Taylor et al. (1981) conducted the experimental examinations to study the anchor-rotation behavior on the placed foundation samples on the sand and clay. The results has been examined for a rectangular shaped foundation sample (0.25m x 0.5m) placed on the context of dry sand. The results of the examinations indicated that the resulted subsidence from the cycle rocking motion is depended to the size, foundation shape, safety factor, sand density and number and the rocking motion domain cycles. Furthermore, the anchor-rotation behavior resulted from the uplift of a corner of the foundation is a nonlinear relation, even if the foundation materials have a liner behavior. Also, in the condition in which the rocking motion domain are large enough to yield the soil under the edge of the foundation, a strong nonlinear anchor-rotation relation with hysteresis damping is observed. This research indicated that the when seismic loading is applied to spread foundations without no serious damage to the vertical loading capacity (this indicates the vertical large safety factor) it may be possible that the rotation surrender is occurred under the foundation. They have recommended that the spread foundations can be designed in the form to bear the severe earthquakes with accepting and preference to columns yield in the ground state in reinforced concrete structures. (8).

Barlett (1973) indicated that the foundation rocking motion and soil yield can change the structure period in different levels. System softening with a large rotation which results in foundation position detachment from the soil can be occurred after soil yield and loss of under foundation soil stiffness. (9).

Wiessing (1979) conducted the (g-1) examination on a shallow foundation sample (0.5 m x 0.5 m) placed on the cohesive soils under the harmonic rocking motion. The results indicated that a progressive subsidence is occurred for the foundation during the rocking motion which alongside this subsidence and simultaneous with the foundation rocking motion a large energy loss is occurred in the soil and the foundation soil will have a plastic deformation. The foundation rocking motion result in its soil sliding as well as cause to system softness reduction by reducing the interface between the foundation and soil. Also, it results in a nonlinear relation for the anchor – rotation. (10).

Zeng and Sttedman (1988) have conducted a series of centrifuge examinations to study the behavior of under seismic loading of the placed buildings on the shallow surface which are placed on the sand. A sudden reduction in loadi capacity in the end of earthquake loading is starting when the earthquake is completely under the maximum value. A clear description of the results indicated that an earthquake with more cycles with average domain which can cause permanent rotation can result in more reduction at foundation loading capacity to the earthquake with only one or two strong cycle. (11). Nuclear Power Engineering Community of Japan (1911) examined the winged thick wall using an earthquake simulator to investigate their response under the dynamic loading until the failure occurrence. 47 simulation analysis have been conducted for the examined walls. 31 of them have been conducted by finite element analysis, 10 of them have been conducted by the simplified models and 6 of them have been conducted by concentrated mass model. The model of the applied concrete in analyzing most of the models have been of crack spread type. The detail of the done

researches were reported in OECD/NEA/CSNI. (12). the result of existing finite element analysis in OECD report indicate that 1) the effect of changes in tensile hardening models on the response is less; 2) most of the estimated values for elastic hardness has 15% difference with the experimental values; 3) the two-dimensioned models in which the wing effective width have been estimated 1000 millimeter resulted the lateral hardness better to the two-dimensioned model considering whole of the wing width (2980 millimeter) 4) The estimated lateral hardness in the simulation which didn't model the wall foundation is similar to the estimated lateral hardness of the simulations in which the wall foundation has been modeled; 5) the maximum shear strength estimated by the finite element analysis calculated between 65 to 115 % of the experimental measured values; 6) the displacement in the maximum shear strength resulted from the analysis calculated between 25 to 185 % of the displacement values in the shear strength; 7) none of the stable crack formulation and the rotary crack formulation were better than each other. (13).

Analyzing the short walls is more difficult than analyzing the slender wall due to the complexity of the shear transfer mechanism in reinforced concrete structures as well as indicate the different fracture types under the seismic loading. So, the designer will face more challenges to predict their seismic behavior in these wall nonlinear analysis. Thus, sampling and analyzing an experimental sample as well as investigating the performance of short shear wall considering the rocking motion has been conducted according to the need to more investigation of the behavioral and analytic aspects of the short shear walls as well as with the aim of achieving a proper tool for analysis based on the performance of these walls.

VALIDATING THE ANALYTICAL MODEL

To analyze, the ATENA 3D finite element analysis software has been applied as follow. This software is suitable for nonlinear analysis of the reinforced concrete structures.

The NUPEC experimental sample wall for the numerical analysis includes five panel (two slab panels, two wing wall and one Jan wall) and two loading plate according to the below characteristics. As, it is observed in Figure 1, the up stab had 4 meter length, 4 meter width and 760 cm height. The down stab had 5 meter length, 5 meter width and 1000 mm height. The Jan wall had 2900 mm length, 2020mm height and 75 mm thickness. The wing walls had had 2980 mm length, 2020mm height and 100 mm thickness. The down stab rebar including a mesh of D29 rebar (29 mm diameter), at the top and bottom of it, the upper slab rebar including a mesh of D25 rebar (25 mm diameter) and the Jan and wing walls of the D6 rebar according to the Figure 2 (13).

The characteristics of the NUPEC experimental sample for numerical analysis has been shown in Table 1.

The material 3D Nonlinear Cementations 2 model is applied for the concrete. This model is a fracture-plastic model i.e. a mixture of fracture characteristic models in the strain and the plastic in the pressure. In this model, the tension softening area is defined by determining the gap energy and the maximum crack width as well as the post-peak pressure area is specified with determining the final strain. (14).

The uniaxial tension-strain curve has been shown in Figure 2 and its relations are as follow;

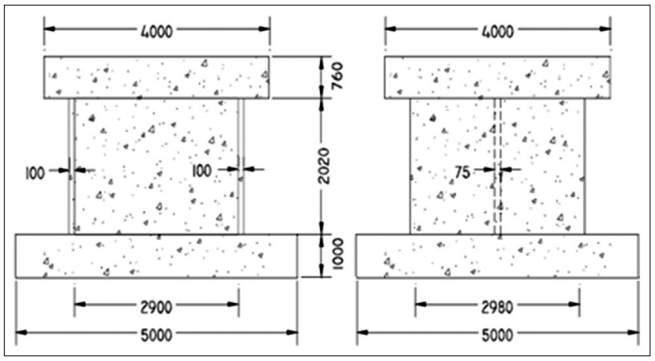

Figure 1: The wall dimensions (13)

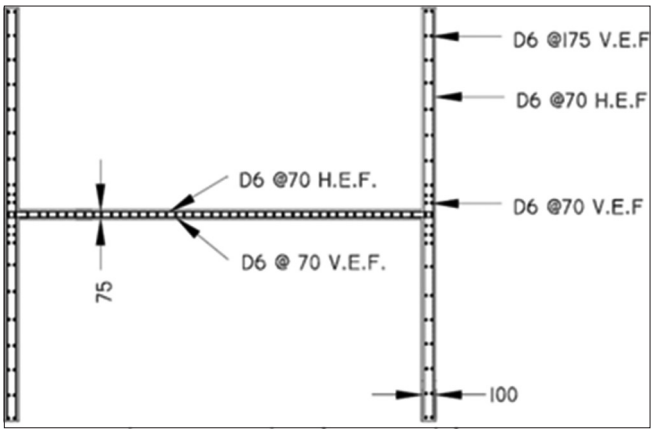

Figure 2: The reinforcing schema (13)

Table 1: Building material characteristics

Rebar characteristics (kg/mm²)			Concrete characteristics (kg/mm²)			
f_u	E	f_y	f_t	*v*	E	f'_c
49.5	18.8×10^3	39.1	0.23	0.155	234	2.92

The ascending pressure part:

$$\sigma_c^{ef} = f_c^{ef} \frac{(E_0 / E_c)(\varepsilon / \varepsilon_c) - (\varepsilon / \varepsilon_c)^2}{1 + [(E_0 / E_c) - 2)](\varepsilon / \varepsilon_c)} \quad (1)$$

$$E_c = f_c^{ef} / \varepsilon_c$$

Where, σc^{ef} is the effective pressure tension of the concrete, fc^{ef} is the effective pressure strength of the concrete, E_0 is the initial elastic modulus of the concrete, Ec is the secant modulus of the concrete in peak tension and ε_c is the strain at peak pressure tension.

The linear descending pressure part:

$$\text{(assumption) } \varepsilon_d = \varepsilon_c + \frac{w_d}{L_d'}, \; w_d = 0.5 m \; m \quad (2)$$

Where, ε_d is the related strain to w_d, the w_d is the plastic displacement at the end of the pressure softening curve, L_d' is the length of rupture band in the pressure.

The linear ascending pressure part:

$$E_c = f_t^{ef} / \varepsilon_t \quad (3)$$

Where, f_t^{ef} is the effective tension strength of the concrete, e_t is the peak elastic tensile stress.

$$w_c = 5.14 \frac{G_f}{f_t^{ef}} \quad (4)$$

The tensile descending part

Where, w_c is the crack width during the full release of tensile stress, G_f the concrete fracture energy (Nmm/mm^2).

The tensile hardening coefficient:

$$\text{(assumption) } c_{ts} = 0.4 \quad (5)$$

Where, c_{ts} is the tensile hardening coefficient.

The biaxial rupture function curve of the concrete has been shown in Figure 3 and its relations are as follow;

The pressure rupture:

$$f_c^{ef} = \frac{1 + 3.65(\sigma_{c1} / \sigma_{c2})}{[1 + (\sigma_{c1} / \sigma_{c2})]^2} f_c \quad \text{Pressure- press} \quad (6)$$

Where, σ_{c1} is the main tension in 1 direction, σ_{c2} is the main tension in direction 2, f_c is the average pressure strength of the concrete cylinder.

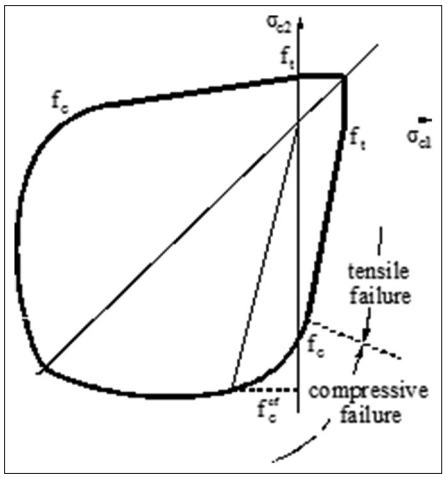

Figure 3: The biaxial rupture function of the concrete (14)

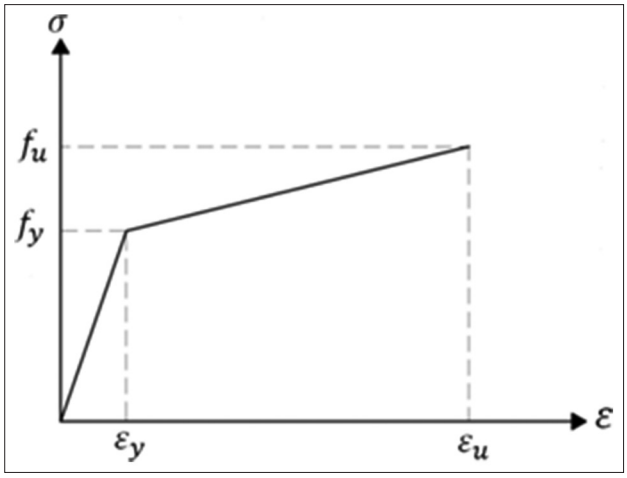

Figure 4: Steel tension-strain curve (15)

The tension- pressure:

$$f_c^{ef} = f_c r_{ec}$$

$$r_{ec} = (1 + 5.3278 \frac{\sigma_{c1}}{f_c}) \quad 1.0 \geq r_{ec} \geq 0.9 \quad (7)$$

Where, r_{et} is coefficient of tensile strength reduction.

The tensile rupture:

$$f_t^{ef} = f_t r_{et}, \; r_{et} = 1 - 0.8 \frac{\sigma_{c2}}{f_c}$$

Pressure-tension (8)

Tension-tension (9)

$$f_t^{ef} = f_t$$

Where, f_t is the uniaxial tensile strength of the concrete.

The pressure and tensile strength of the concrete and its elastic modulus have been achieved by the examination. Concrete fracture energy is achieved by the below relation;

$$G_f = 0.025 (f_c / 10)^{0.7} \quad (10)$$

ATENA applies the (smeared) distribution crack model with two different option, stable crack model and rotation crack model. In both of the models, the crack is arisen when the main tension is more than tensile strength. It is assumed that are distributed uniformly in the material volume. This reality is arisen with the definition of Orthotropia in the determined model. In the stable crack model, the crack direction and the main tension direction at the crack arisen moment is determined. This direction is stable continuing the loading and indicated the Orthotropia axial of the materials, the direction of the tensions and main strains in the cracked concrete matches each other due to the concrete isotopic assumption. In the rotation crack model, the direction of the main tensions matches the direction of the main strains. The crack direction rotates while the rotation of the main strains. The user can change the distribution crack from the rotation model to the stable model. The numerous analysis with the different stable crack values (the ratio of the tensile tension to the tensile strength in the mode of change to stable crack) indicated that the full stable crack model creates better results. The full plastic-elastic bilinear model applied for the rebar. The CEB-FIP Model code 90 cohesion- sliding model has been considered for the rebar cohesion to the concrete. (15). the tension-strain curve has been shown in the Figure 4. The hardening bilinear model has been applied for the rebar. (15).

According to the existence of the hooks, the zero sliding is considered for the both sides of the rebar. The meshing of the analytical model is shown in the Figure 5.

In the first step of the loading, the parts weights have been applied. Then, the additional axial power has been applied to the upper level of the above slab in the form of incremental monotonic. The sum of the applied axial load and above slab was 1220KN which was stable at the next steps of the loading. The lateral load has been applied to the construct in 20 phases in the form of incremental replacement control in the center of the above slab.

The other part of ATENA3D software is the easier method to solve the nonlinear equations by the finite element method and incremental loading criteria. Different ways are existed in this software to solve the nonlinear equations. The Newton-Raphson method in combination with the linear search method along with updating the hardness matrix in each step has been applied to solve the nonlinear equations system. The waste and absolute errors were 0.02 and 0.05, respectively. Maximum 40 repeats were considered in each step.

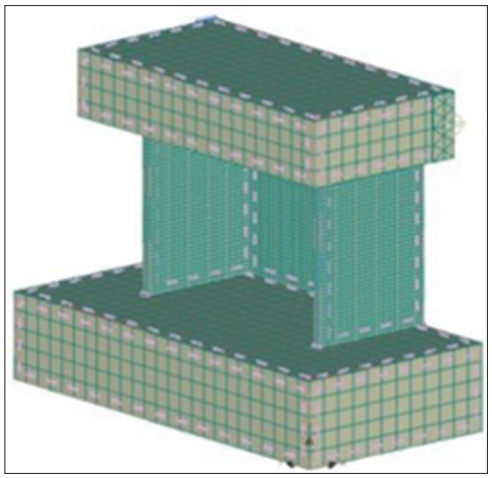

Figure 5: The meshing of the analytical model, the place of loading and measuring the lateral displacement

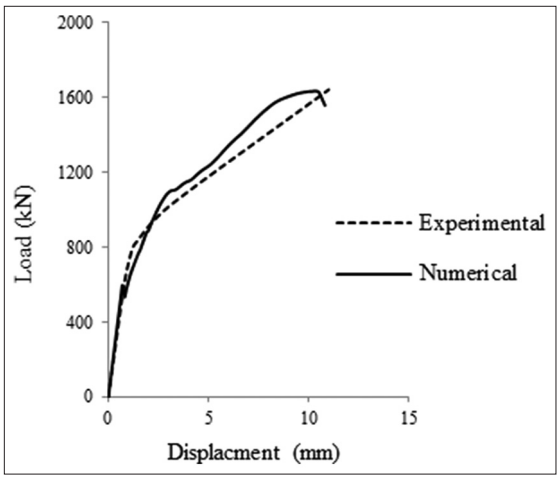

Figure 6: The displacement-load curve at the wall upper point

The cover of cyclic curves has been shown in Figure 6 (for better comparison, the units has turned to the presented units in the examination.

Cycle of drift applied is exactly similar to the experimental sample. According to Table 2, the shear resistance of the maximum wall resulted from analysis was 1639 kilo newton in 10.43mm displacement.

By comparing the achieved curves and the analytic and experimental results, it has been observed that there is a good match between two results.

Table 2: Evaluation of placement and tensile strength

Sample	$V_{U\,Num.}$(kN)	V_U Exp.(kN)	$\frac{V_{UNum.}}{V_{UExp.}}$ (kN)	Placement of analytical sample (mm)	Placement of laboratory sample (mm)	$\frac{\text{Placement of analytical sample}}{\text{Placement of laboratory sample}}$
NUPEC	1639	1641.76	0.9983	10.43	10.98	0.9499

THE CONVENTIONAL SHORT WALLS IN RETROFITTING

With the aim of providing the different approaches in facing with all types of buildings in the different risk levels, the seismic retrofitting functional guidelines was presented by the International Institute of Earthquake Engineering and Seismology. To retrofit the short buildings, a sample of rectangular shear wall which placed on the strip foundation has been presented. To investigate the effective parameters on this kinds of behavior and improving their performance, these walls have been modeled numerically and under the incremental lateral loading (nonlinear static analysis) using the mentioned findings. The dimension of the proposed wall plan dimensions has been shown in Figure 7 and the lateral side and its section has been shown in Figure 8. The characteristics of the used materials and the wall baring have been shown in Tables 3 and 4.(16).

Concrete and steel models have been considered as the Figures 9, 3 and 6, then the lateral loading has been applied to that in the form of displacement control and with the incremental stable rhythm.

4. For foundations with rocking motion, soil with bed coefficient of 2 (kg/m^3) was modeled as spring and permissible soil resistance was assigned 2 for every condition and tensile strength of soil spring was considered as zero. Form and output of analysis for foundation with rigid abutment and rocking motion are represented in Figures 10-12 and 13-15; respectively.

As can be seen in Figure 11, destruction modes is mainly of shear type with sudden drop after the peak and remaining resistance was about 14% of the maximum resistance.

According to graphs 11 and 14, maximum tensile strength for model with rigid abutment KN1444was 10.4mm in placement and for model with rocking motion 261.4KN was 19.5mm. Figure 12 shows remaining tensile strength and determines direction and angle of the cracks. As seen, critical crack was relatively horizontal and close to the wall.

In rocking motion, foundation makes progressive rocking motion around the beneath soil and this rotation motion reduces contact area between soil and foundation

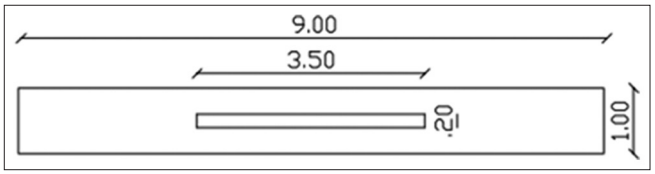

Figure 7: Wall plan (11)

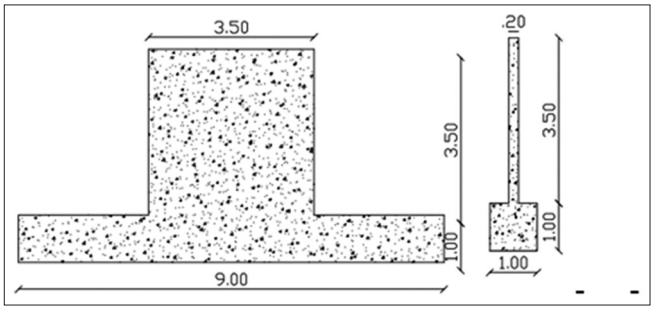

Figure 8: The lateral side and wall section (11)

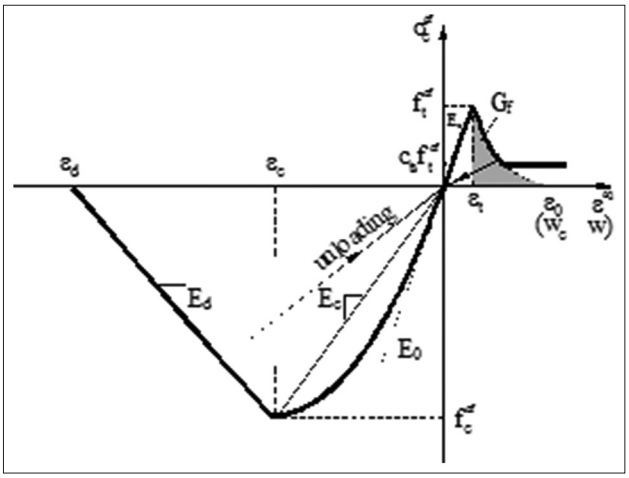

Figure 9: The uniaxial tension-strain of the concrete (14)

and hence results in non-linearity of soil pressure distribution. Non-linearity of the pressure together with the change in contact area results in non-linearity and reduction of moment-rotation. Therefore, bending moment is achieved at lower levels of rotation and even by increase in rotation rate, moment is reduced slightly. When soil contact area under the foundation yields and upright loading capacity is transferred, foundation continues its rotation without any change in bending moment rate. A considerable volume of energy is lost at soil-foundation contact area.

EVALUATING SOIL-FOUNDATION INTERACTION IN LATERAL LOAD

Soil stress under rigid foundations under gravity load and bending moment is linear. Thus the stress below shear wall foundation under low lateral load is trapezoidal. By increase in lateral force, moment on the foundation is elevated so that soil stress under foundation reaches zero in one extreme. By further increase in lateral force, a part of the foundation gets detached from the soil and soil stress becomes zero. If only gravity force is exerted on

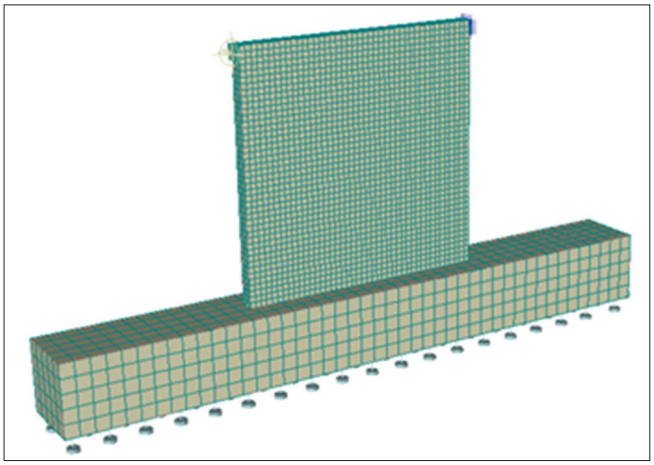

Figure 10: Model with rigid abutment

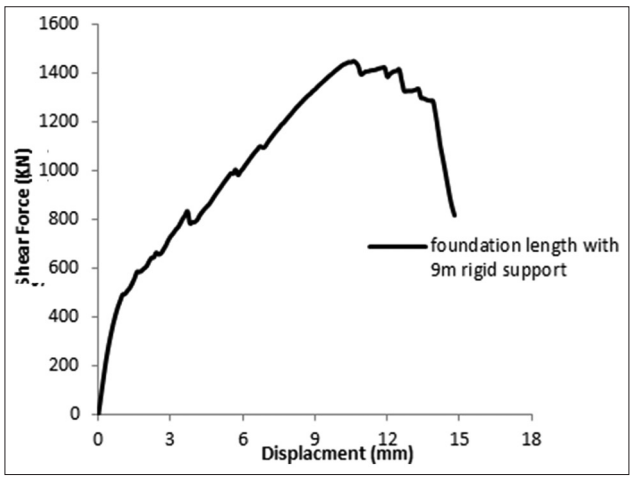

Figure 11: Graph of placement load of wall with rigid abutment

Table 3: Properties of wall and materials

L_w(m) wall	H_w(m) wall	t_w(cm) wall	F_c'(kg/cm²)	F_y(kg/cm²)	Rebar
3.5	3.5	20	210	4000	A III

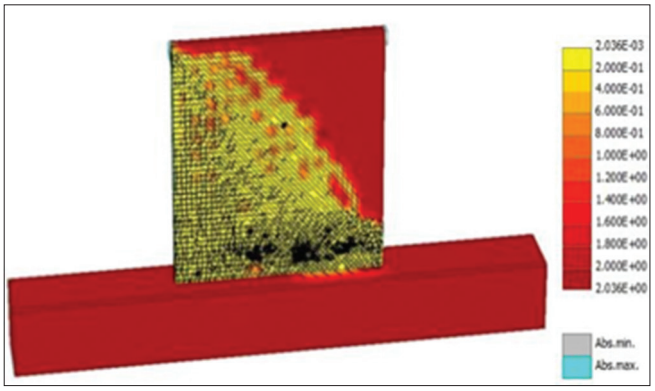

Figure 12: Distribution of tensile strength and final crack with rigid abutment

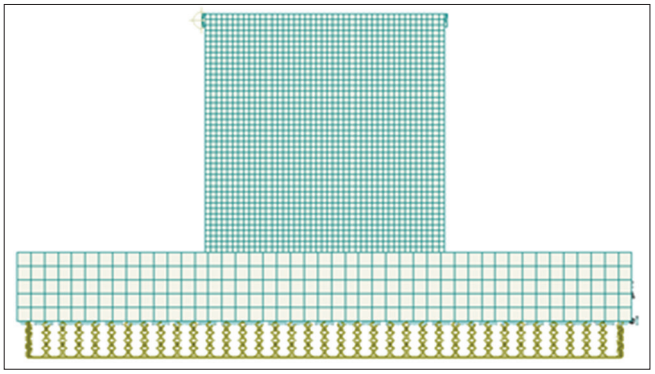

Figure 13: Model with rocking motion

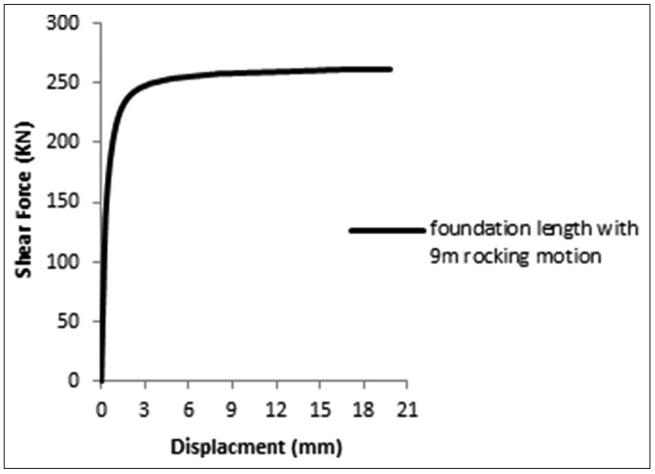

Figure 14: Placement load of wall with rocking motion

Table 4: Properties of reinforcement and foundation

Upright reinforcement of the wall	horizontal reinforcement of the wall	Foundation section (m)	Foundation length (m)	Longitudinal reinforcement of the foundation	Latitudinal reinforcement of the foundation
∅20@25	∅16@25	1×1	9	∅257	∅20@20

the center of a foundation, soil stress is distributed evenly; however, if bending moment is also exerted, then the stress is distributed unevenly so that soil pressure stress is concentrated in one side of the foundation. Bending moment causes triangular uneven distribution of the stress within the soil. Distribution area of this stress is equal to upright force exerted to the foundation. The distance between stress distribution center and the point on which the upright load is exerted causes formation of a resistant moment that should be in dynamic balance with the moment exerted on the foundation.

EFFECT OF REBAR ARRANGEMENT AND AXIAL DAM ON PERFORMANCE OF SHORT SHEAR WALL

Ghanizadeh et al (2014) investigated the role of diagonal rebar on wall behavior to promote wall formability. Double diagonal reinforcing bars with different numbers were used. As can be seen in Figures 16-18, with equal loading capacity, sliding shear placement is decreased by increase in lateral placement which promotes energy absorption in short shear wall and the role of diagonal rebar in tensile strength is elevated and by increase in rebar diagonal, final tensile strength is increased and formability is reduced. By placing diagonal rebar 12 in both sides of the wall, placement in peak point is increased by 33% (17).

According to Figure 18, more than half of the wall works with tensile and by increase in rebar diameter, cracking area is extended.

Ghanizadeh et al (2014) used axial load of 0.2 $f'_C A_g$, 0.3 $f'_C A_g$ and 0.4 $f'_C A_g$ to investigate the effect of axial load on models' formability. According to Figures 19 and 20, by increase in axial force, tensile strength is increased and ductility is decreased. In winged sample, by increase in axial load to P_U=0.2 $f'_C A_g$ final shear strength is increased by 31% and in rectangular sample, by increase in axial load to P_U=0.4 (f'_C) A_g, final shear strength is increased by 70% [18].

For P_U=0.2 $f'_C A_g$

According to Figure 20, more than half of the wall has reached its tensile strength. Rupture is seen at the end of the wall and also at the left upright edge.

EFFECT OF FOUNDATION ON PERFORMANCE OF SHORT SHEAR WALL

Using geometrical coordination depicted in Figure 21, effect of short shear wall along the foundation was evaluated for lengths including 3.5m, 5.5.m, 7.5m, 9m, 11.5m and 13.5m.

Figure 22 shows placement of wall with rigid abutment and with rocking motion in a 3.5m foundation.

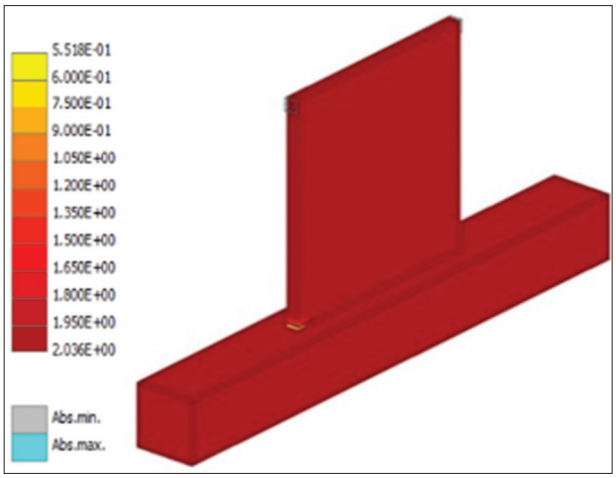

Figure 15: Distribution of tensile strength and final crack with rocking motion

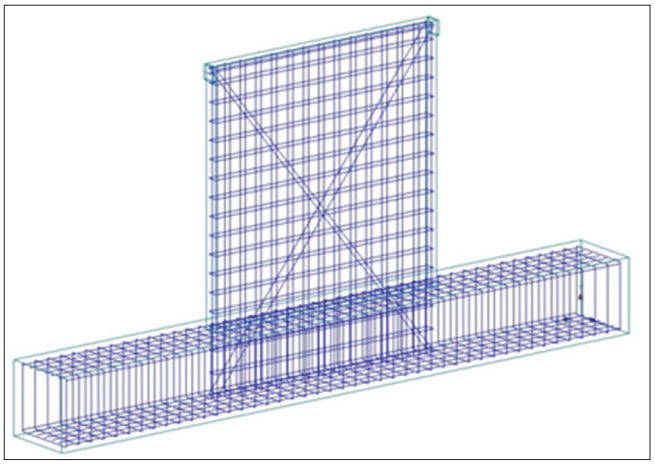

Figure 16: Diagonal reinforcement plan

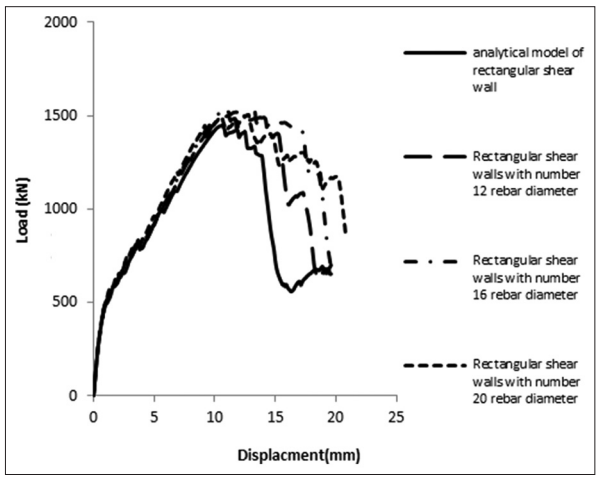

Figure 17: Model analysis based on diagonal reinforcement

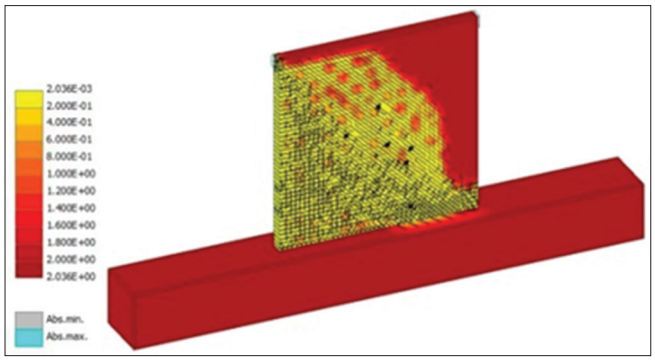

Figure 18: Distribution of tensile strength and final crack for rebar 12

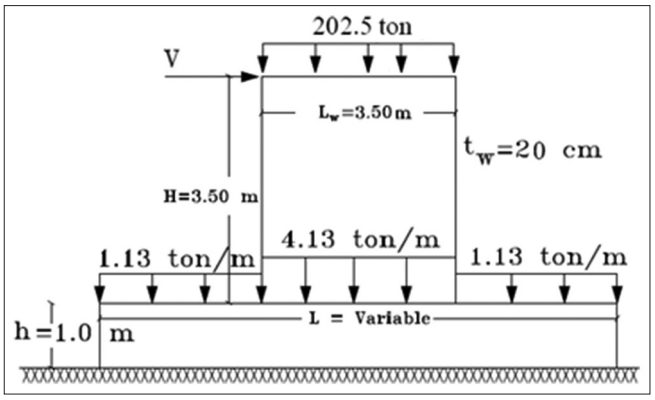

Figure 21: Geometrical specifications of the model

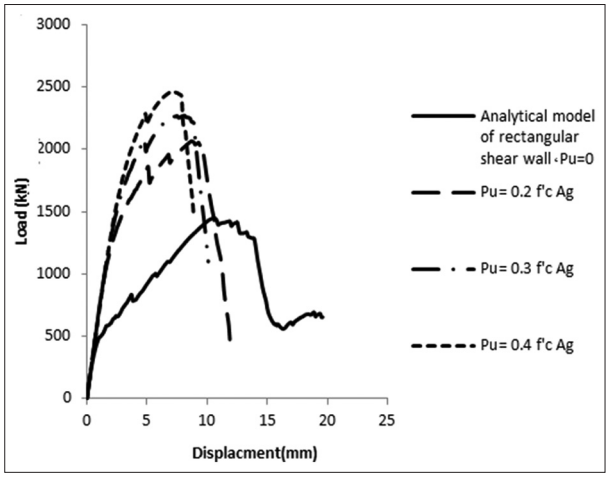

Figure 19: Model analysis based on axial load

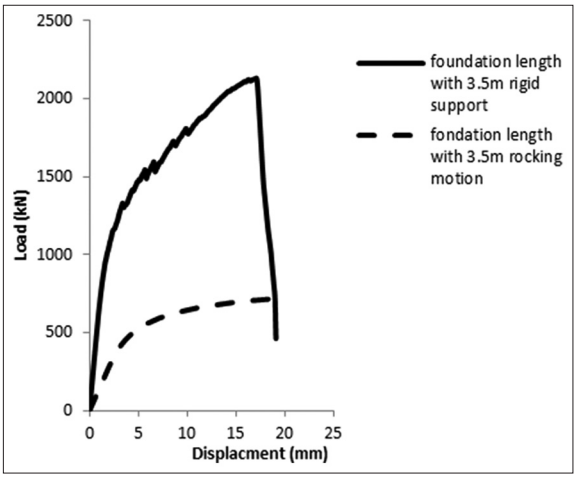

Figure 22: Model analysis for 3.5 m foundation

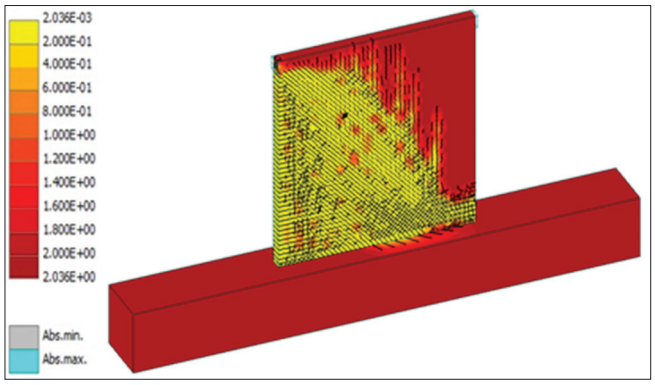

Figure 20: Distribution of tensile strength and final crack

According to Figure 22, by removing the stanchion and occurrence of rocking motion, tensile strength is reduced by 64% and after a 5mm placement; foundation begins rotation as a rigid body. Final analyses of a 3.5m foundation are depicted in Figures 23-25.

According to Figure 23, wall rupture mode is shear type and Figure 24 shows flowing of longitudinal and latitudinal rebar.

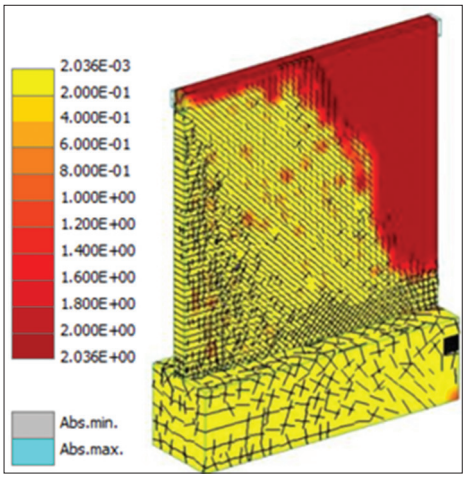

Figure 23: Distribution of tensile strength and final crack for rigid abutment

According to Figure 25, material behavior remains in elastic area and no bending crack occurs in the wall; confirming rigid body rotation. Cracking mode and flowing of tensile steels in the wall with rigid foundation for lengths of 5.5m, 7.5m, 9m, 11.5m and 13.5m are shown in Figures 23 and 24.

According to Figure 26, by removing the stanchion and occurrence of rocking motion, tensile strength is reduced by 35% and its formability is doubled. Final analyses of a 5.5m foundation are depicted in Figures 27 and 28.

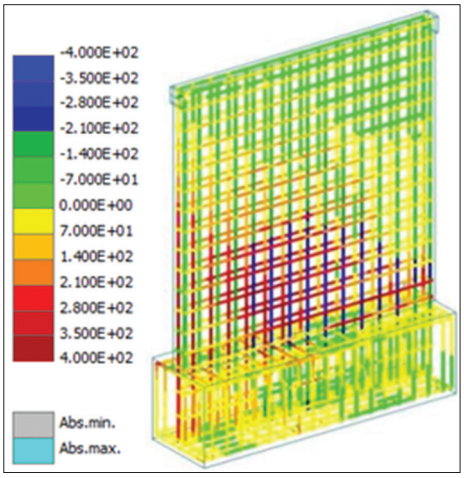

Figure 24: Distribution of final stress for rebar with rigid abutment

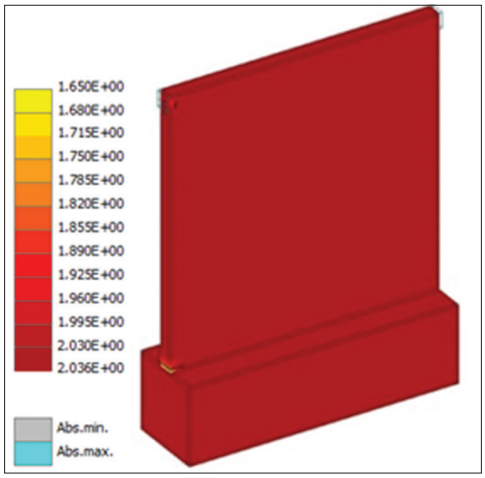

Figure 25: Distribution of tensile strength and final crack for rocking motion

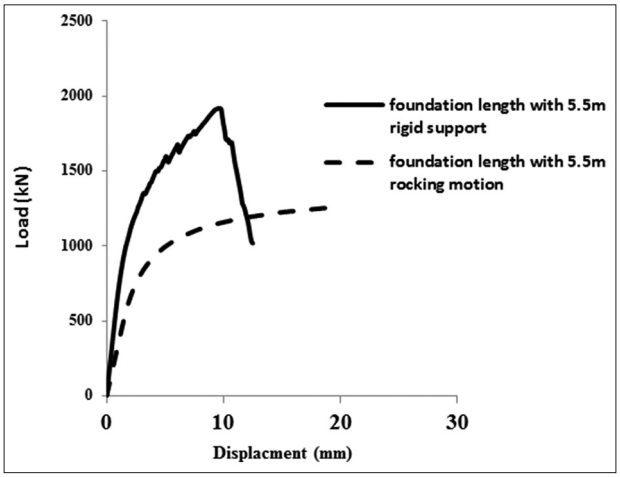

Figure 26: Model analysis for 5.5 m foundation

Figure 27 shows that tension has occurred in lower left part of the wall; but the wall has not used its final capacity yet.

According to Figure 28, rebar has reached flowing limit in corner of tension dimension in two upright rows. Figure 29

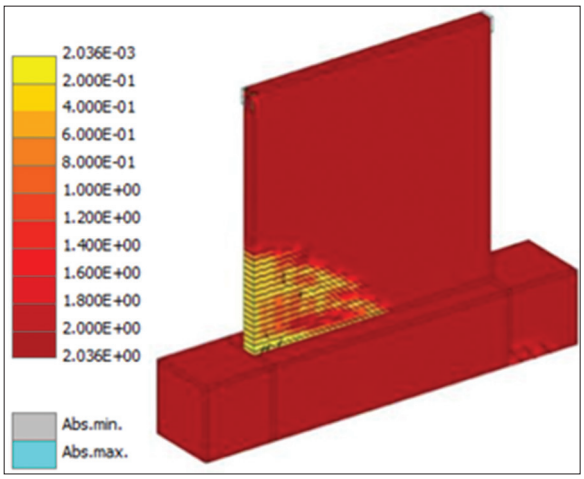

Figure 27: Distribution of tensile strength and final crack for rocking motion

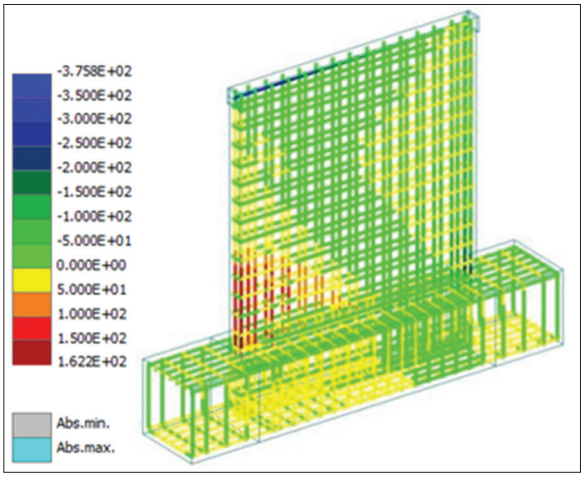

Figure 28: Distribution of final stress for rebar with rocking motion

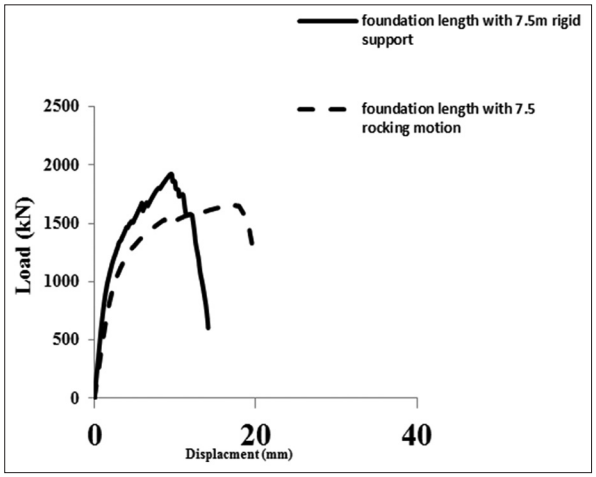

Figure 29: Model analysis for 7.5 m foundation

represents load-placement graph of the wall with rigid abutment and rocking motion in a 7.5m foundation.

According to Figure 29, by removing the stanchion and occurrence of rocking motion, tensile strength is reduced by 24% and its formability is doubled. Final analyses of a 7.5m foundation are depicted in Figures 30 and 31.

According to Figure 30, more than half of the wall and pressure zone of the wall is subjected to tension and the crack has been extended in lower left and right parts of the wall.

Figure 31 indicates that horizontal and upright rebar in tension dimension of the wall together with some shear rebar in the foundation have reached flowing limit. Figure 32 represents load-placement graph of the wall with rigid abutment and rocking motion in a 9m foundation.

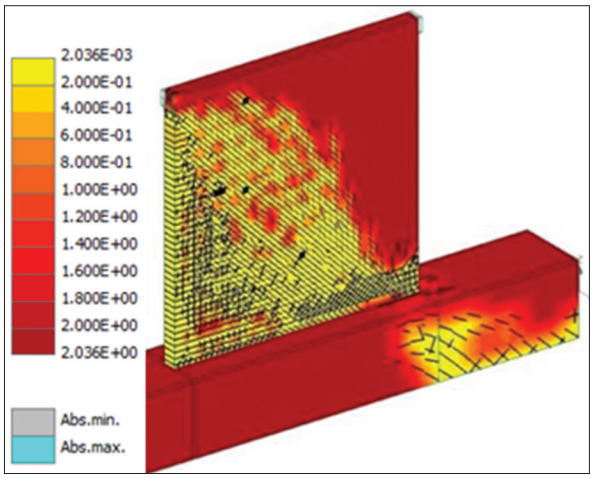

Figure 30: Distribution of tensile strength and final crack for rocking motion

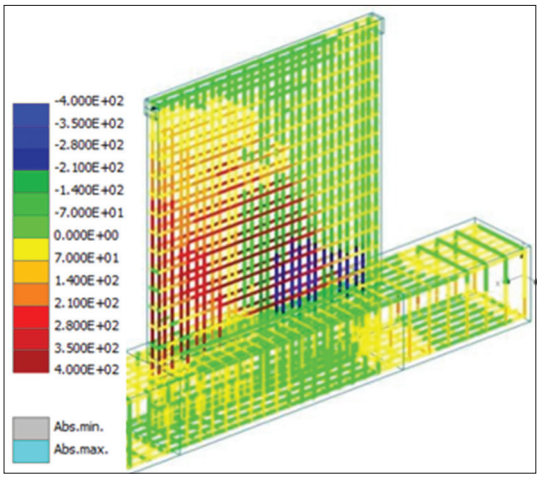

Figure 31: Distribution of final stress for rebar with rocking motion

According to Figure 32, by removing the stanchion and occurrence of rocking motion, tensile strength is reduced by 11% and its formability is increased by 20%. Final analyses of a 9m foundation are depicted in Figure 33.

According to Figure 33, most of the wall and lower pressure zone of the wall is subjected to tension and the crack has been extended in in tension and pressure dimension of the wall and also in lower pressure zone of the foundation. Figure 34 represents load-placement graph of the wall with rigid abutment and rocking motion in 11.5m foundation.

According to Figure 34, by removing the stanchion and occurrence of rocking motion, tensile strength is reduced by 8% and its formability is increased by 12%. Final analyses of a 11.5m foundation are depicted in Figure 35.

According to Figure 35, more than half of the wall is subjected to tension and the rupture has occurred in tension dimension and wall base while crack occurs in

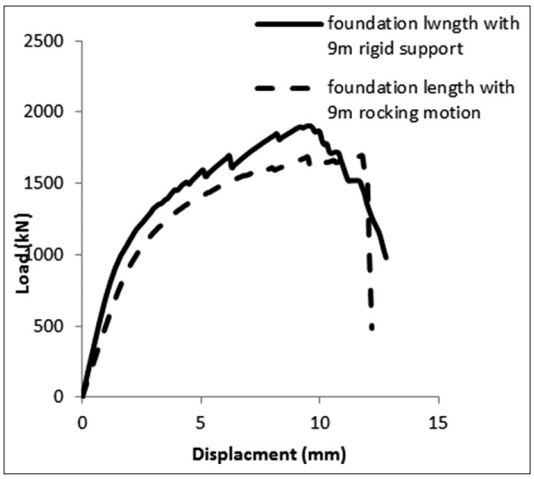

Figure 32: Model analysis for 9 m foundation

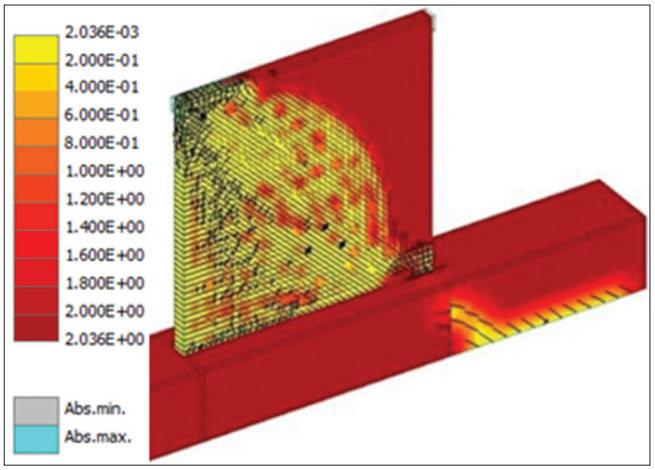

Figure 33: Distribution of tensile strength and final crack for rocking motion

Table 5: Results of samples' analysis

	Final tensile strength	Placement	Tensile strength Sample with rocking motion / sample with rigid abutment	Placement Sample with rocking motion / sample with rigid abutment
Sample with rigid abutment (L=3.5m)	2125	16.9	0.341	1.45
Sample with rocking motion (L=3.5m)	725.3	24.6		
Sample with rigid abutment (L=5.5m)	1918	9.49	0.65	2.06
Sample with rocking motion (L=5.5m)	1259	19.6		
Sample with rigid abutment (L=7.5m)	1904	9.19	0.86	1.90
Sample with rocking motion (L=7.5m)	1656	17.5		
Sample with rigid abutment (L=9m)	1899	9.39	0.89	1.24
Sample with rocking motion (L=9m)	1692	11.7		
Sample with rigid abutment (L=11.5m)	1940	9.69	0.92	1.12
Sample with rocking motion (L=11.5m)	1793	10.9		
Sample with rigid abutment (L=13.5m)	1913	9.59	0.95	1.14
Sample with rocking motion (L=13.5m)	1820	11		

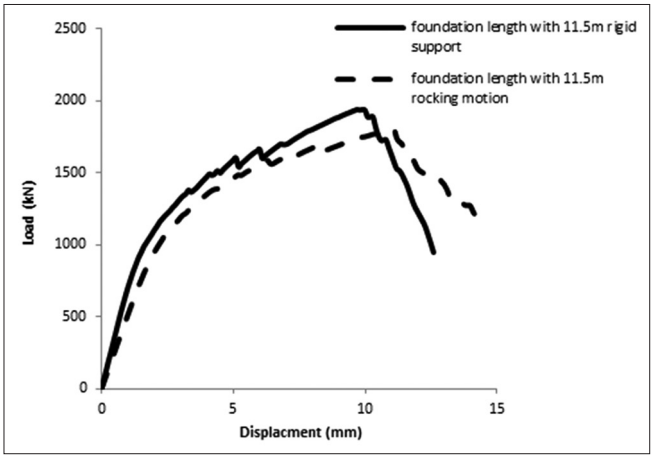

Figure 34: Model analysis for 11.5 m foundation

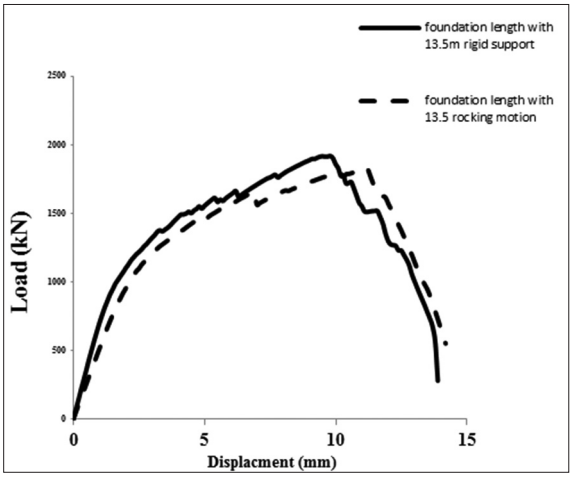

Figure 36: Model analysis for 13.5 m foundation

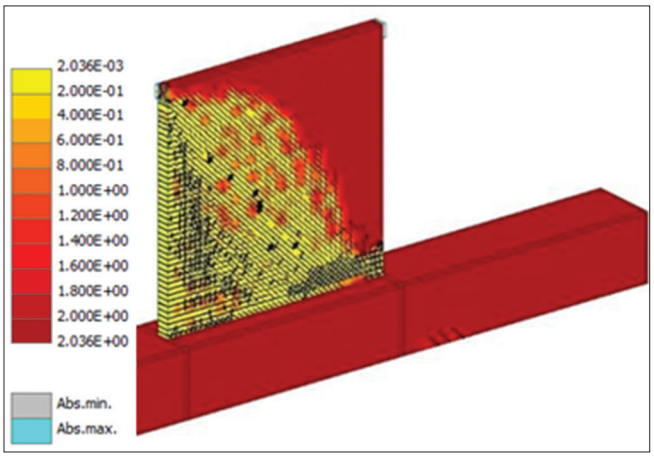

Figure 35: Distribution of tensile strength and final crack for rocking motion

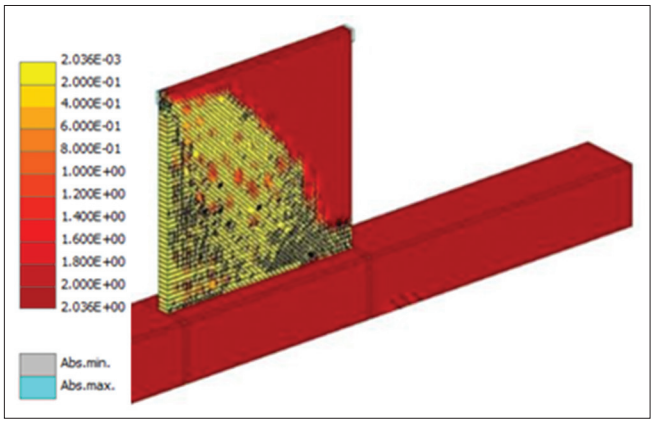

Figure 37: Distribution of tensile strength and final crack for rocking motion

pressure zone of the foundation close to the wall. Figure 36 represents load-placement graph of the wall with rigid abutment and rocking motion in a 13.5m foundation

According to Figure 36, by removing the stanchion and occurrence of rocking motion, tensile strength is reduced by 5% and its formability is increased by 14%. Final analyses of 13.5m foundation are depicted in Figure 37.

The results of samples' analysis are represented in Table 5.

CONCLUSION

In this study, small shear walls with rectangular cross-section, with an aspect ratio of height to length equal to one, the compressive strength of 21 (kg/cm ^ 2) and even lateral load used by International Institute of Earthquake Engineering and Seismology to strengthen short structures was investigated. Impact of short shear wall performance, taking into account the effect of rocking motion of a rigid support, on the ultimate strength and formability of shear walls were studied and the results were as follows:

If high strength is not expected from the wall, flexible behavior of the wall based on rocking motion can be used to improve construct's formability. If the foundation is completely rigid, then soil stress diagram below the foundation will be linear; whereas the diagram is non-linear in foundations with rocking motion.

By increasing the length of the foundation in the rocking motion, the behavior of shear wall behavior moves from flexible to rigid behavior, shear strength and stiffness of the structure is increased while formability is reduced. With the increase in foundation length from 3.5 m to 7.5 m, lateral bearing capacity, is increased almost by 2.5 times and formability of wall compared to rigid status is increased by about 90 percent. With the increase in length from 7.5 m to 13.5 m, lateral loading capacity was increased only 10%. For foundation with more than 9m length, tensile strength and yield placement of the shear wall with the rocking motion is close to that of wall with rigid abutment.

REFERENCES

1. Barlett, P. E. (1976). "Foundation Rocking on a Clay Soil". M E Thesis University of Auckland School of Engineering, Report No. 154.
2. Cervenka, V., Jendele, L., Cervenka, J., (2007). "ATENA Program Documentation, Part 1, Theory".Cervenka Consulting, Prague, August 23,pp. 231.
3. Comite Euro-International du Beton. (1993). "CEB-FIP Model Code 1990". Bulletins d'Information 203-205, CH-1015 Lausanne, pp. 437.
4. FEMA 274. (1997). "NEHRP Commentary of the Guidelines for the Seismic Rehabilitation of Buildings". Prepared by the Applied Technology Council with funding from the Federal Emergency Management Agency, Washington, D.C.
5. FEMA 440. (2005). "Improvement of Nonlinear Static Seismic Analysis Procedures". Prepared by the Applied Technology Council for the Federal Emergency Management Agency, Washington, D.C.
6. Ghanizadeh, M., Sarvghad, A., Farzam, M. effect of rebar arrangement on seismic performance of small shear-walls; journal of engineering modeling, 2014.
7. Ghanizadeh, M., Sarvghad, A., Farzam, M. effect of axial load and materials properties on seismic performance of small shear-walls; journal of engineering modeling, 2014.
8. Georgiad, M. (1985). "Load Path Dependent Stability of Shallow Foundations". Soilsand Foundations, Vol. 25, No. 1,pp. 84-88.
9. Georgiad, M., Butterfield, R. (1988). "Displacements of Footings on Sand Under Eccentric and Inclined Loads". Canadian Geotechnical Journal, Vol. 25, pp. 199-21.
10. Gottardi, G., Butterfield, R. (1993)." On the Bearing Capacity of Surface Footings on Sand under General Planner Loading". Soils and Foundations, Vol. 33, No. 3,pp. 68-79.
11. Gottardi, G., Butterfield, R. (1995). "The Displacement of a Model Rigid Surface Footing on Dense Sand under General Planar Loading" Soils and Foundations, Vol. 35, No. 3,pp.71-82.
12. Gottardi, G., Houlsby, T., Butterfield, R. (1999). "Plastic Response of Circular Footingson Sand under General Planer Loading". Geotechnique, Vol. 49, No. 4, pp.453-469.
13. International Institute of Earthquake Engineering and Seismology (2011). Practical manual for seismic optimization; technical features and executional details according to shear wall; spring, no. 10290/2-2266.
14. Nuclear Power Engineering Corporation of Japan (NUPEC). (1996). "Comparison Report, Seismic Shear Wall ISP, NUPEC's Seismic Ultimate Dynamic Response Test". Report No. NU-SSWISP-D014, Organization for Economic Co-Operation and Development, Paris,pp. 407.
15. OECD NEA CSNI, Shear Wall ISP NUPEC's Seismic Ultimate Dynamic Response Test Comparison Report. Issy Les Moulineaux. France.ReportNo. OCDE GD(96)188.Committee on the Safety of Nuclear Installations OECD Nuclear Energy Agency,(1991), pp.412.
16. Taylor, P. W., Barlett, P. E., Wiessing, P. R. (1981). "Foundation Rocking under Earthquake Loading". Proc of the 10th Intl Conf on Soil Mechanics and Foundation Engineering, Vol. 3,pp. 322-333.
17. Wiessing, P. R. (1979). "Foundation Rocking on Sand". M E Thesis University of Auckland, School of Engineering, Report No. 203.
18. Zeng, X., Steedman, R. S. (1998). "Bearing Capacity Failure of Shallow Foundations in Earthquakes". Geotechnique, Vol.48, No. 2, pp.235-256.

How to cite this article: Ghanizadeh M, Farzam M, Ghanizadeh E. Studying the Performance of Short Shear-Walls Considering Rocking Motion Effect. Int J Sci Stud 2017;5(4):514-526.

Source of Support: Nil, **Conflict of Interest:** None declared.